Electronic Supplementary Material (ESI) for Physical Chemistry Chemical Physics.
This journal is © the Owner Societies 2024

Supporting information

Conformational control of antimicrobial peptide amphiphilicity: Consequences for boosting membrane interactions and antimicrobial effects of photocatalytic TiO_2 nanoparticles

Lucrezia Caselli[*1], *Sebastian Köhler*[2], *Davide Schirone*[3], *Ben Humphreys*[4], *Martin Malmsten*[1,5]

[1]Department of Physical Chemistry 1, Lund University, SE-22100 Lund, Sweden

[2]LINXS Institute of Advanced Neutron and X-ray Science, Scheelevagen 19, 22370 Lund, Sweden

[3]Department of Biomedical Sciences and Biofilms-Research Center for Biointerfaces (BRCB), Malmö University, 20506 Malmö, Sweden

[4]Institut Laue–Langevin, CS 20156, 38042 Grenoble Cedex 9, France

[5]Department of Pharmacy, University of Copenhagen, DK-2100 Copenhagen, Denmark

[*]Corresponding author

KEYWORDS: Antimicrobial peptide, conformation, membrane, nanoparticle, photocatalysis, TiO_2

Scheme S1. Schematic illustration of the model applied to fit the NR data. For lipid PC and +PG bilayers, a 4-layers model was employed, with a water layer in between the bilayer and the quartz surface (1), followed by an inner polar headgroup (2), a hydrophobic tails (3), and a outer polar headgroup (4) layer. The model assumes a homogeneous lateral distribution (i.e., over the bilayer plane) of the different lipid species and identical structural and compositional features for the inner and outer lipid polar headgroup layers.

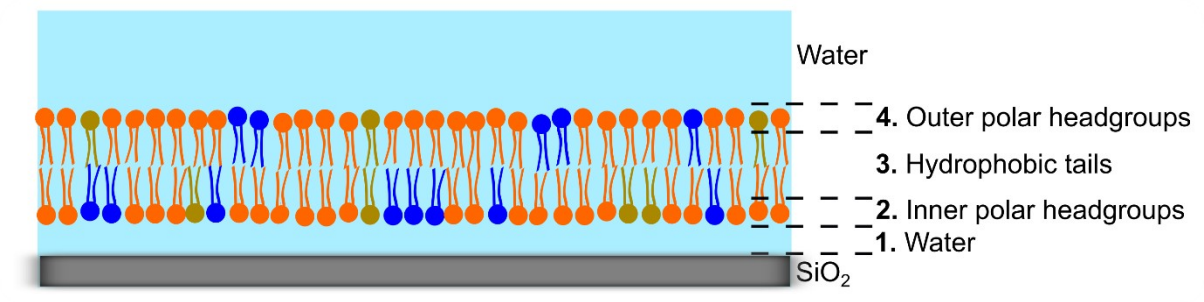

.

Table S1. Input parameters used in the NR fits for the PC and the +PG bilayers. Structural parameters for the different lipids are based on literature values for areas and volumes of full acyl chains or fragments of these, assuming the same volumes for each hydrocarbon group, i.e., =CH, -CH_2, or CH_3, for all acyl chain types (1). All SLD values were calculated from the molecular volumes and nuclear scattering lengths. For POPG, the variation in head group SLD in the different contrasts (d-, qm- and h-buffer), due to partial hydrogen exchange, was considered. The remaining SLD values were calculated from the molecular volumes and nuclear scattering lengths to 4.18 for quartz, -0.56 for the h-buffer, 6.1-6.3 for the d-buffer, and 4.18 for the qm-buffer, all expressed as 10^{-6} Å^{-2}.

Parameters	**POPC**	**PAPC**	**POPG**
Molecular volume (Å^3)[a]	1255	1277	1181
Head volume (Å^3)	331[b]	331[b]	257[c]
Tail volume (Å^3)[d]	924	946	924
Head SLD (10^{-6} Å^{-2})[e]	1.82	1.82	2.5 (h) 2.8 (qm) 3.2 (d)
Tail SLD (10^{-6} Å^{-2})[e]	-0.306	-0.065	-0.306

a: calculated as $v_{total} = v_{tail} + v_{head}$.

b: from (2)

c: from (3)

d: calculated as $v_{tail} = n_{CH_2} \cdot 27.6 + n_{CH=CH} \cdot 44.2 + n_{CH_3} \cdot 53.6$; based on (1).

e: calculated as $SLD = \frac{\Sigma(N_i \cdot b_i)}{V_m}$

Table S2. Summary of structural data obtained from NR fits for PC and +PG bilayers before and after 20 ppm EFK17-W-TiO_2 NP deposition, as well as after 2 h of *in situ* UV exposure. Input parameters (i.e., SLD values and head group thicknesses (Thick)) are shown in bold, fixed and assumed constant. Shown also are fitted structural parameters, including thickness (Thick), hydration (Hyd), roughness (Rough) for each head and tail layer, area per molecule (APM), and surface coverage (Γ). These parameters were obtained fitting the NR profiles by using the Genetic Optimization method the available on the analysis package Motofit within the software IGOR Pro (4,5), according to a 4-layers model (**Scheme S1**). A Monte Carlo error analysis allowing for refitting data 100 times was employed to minimize the uncertainty associated to data fitting (6).

		Head groups				**Acyl chains**				Total Thick (Å)	APM (Å^2)	Γ (mg/m^2)
		SLD (10^{-6} Å^{-2})	Thick (Å)	Hyd (%)	Rough (Å)	SLD (10^{-6} Å^{-2})	Thick (Å)	Hyd (%)	Rough (Å)			
PC	Initial	**1.82**	**7.5**	32 ± 3	7 ± 1	**-0.23**	28.2 ± 0.3	0.20 ± 0.05	7 ± 1	43 ± 1	63 ± 4	4.03 ± 0.07
	+EFK17 -W-TiO_2			30.4 ± 0.3	7 ± 1		23.6 ± 0.1	0.10 ± 0.05	7 ± 1	39 ± 1	66 ± 4	3.80 ± 0.05
	+2h UV			31 ± 1	8 ± 1		22.4 ± 0.1	0.30 ± 0.05	8 ± 1	37 ± 1	68 ± 5	3.70 ± 0.05
+PG	Initial	**2.00** (h) **2.1** (qm) **2.17** (d)	**7.5**	34 ± 2	7 ± 1	**-0.23**	29.2 ± 0.2	0.20 ± 0.02	8 ± 1	44 ± 1	63 ± 4	4.00 ± 0.06
	+EFK17 -W-TiO_2			37 ± 1	7 ± 1		22.4 ± 0.1	0.30 ± 0.01	8 ± 1	37 ± 1	72 ± 4	3.50 ± 0.05
	+2h UV			41 ± 1	9 ± 1		19.2 ± 0.2	34.0 ± 0.1	8 ± 1	34 ± 1	96 ± 4	2.60 ± 0.05

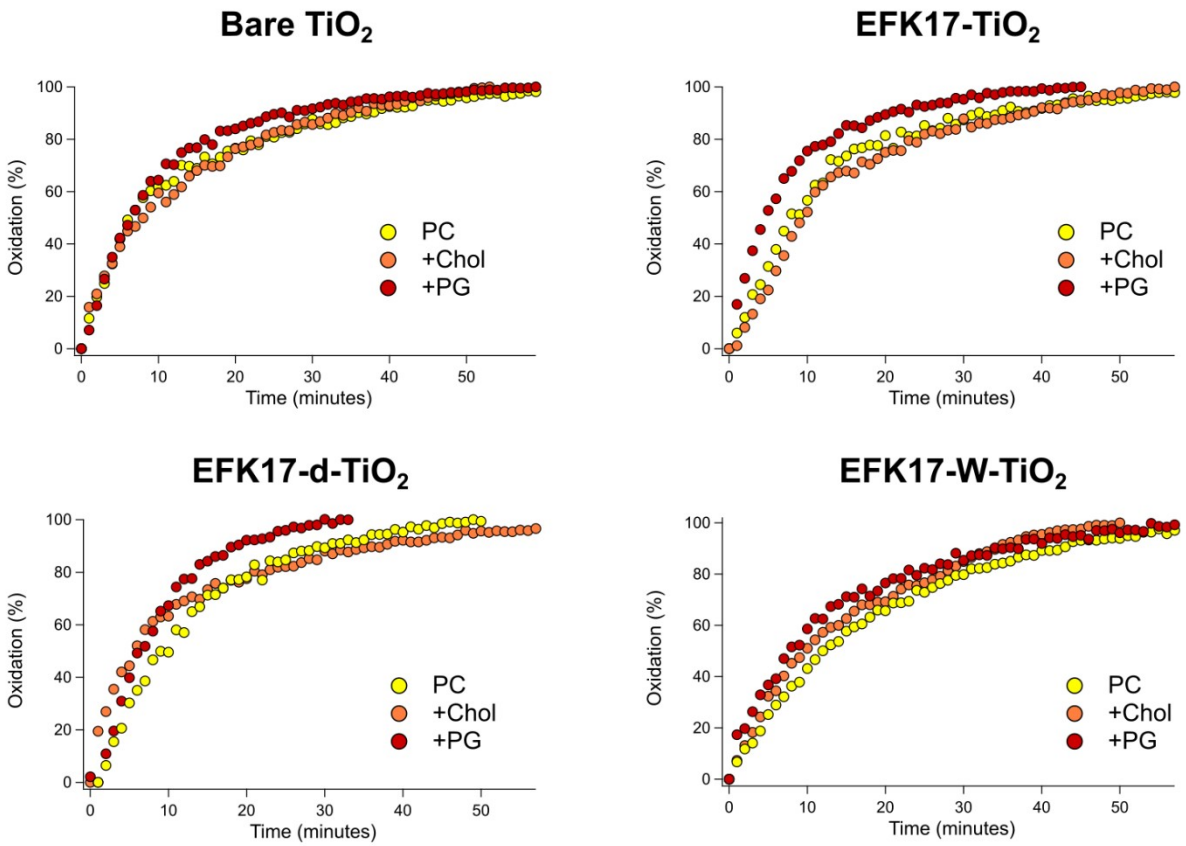

Figure S1. C_{11}-BODIPY oxidation kinetics, showing the effect of 100 ppm bare TiO_2 (top left), EFK17-TiO_2 (top right), EFK17-d-TiO_2 (bottom left) and EFK17-W-TiO_2 (bottom right) for +PG, +Chol and PC LUVs subjected to *in situ* UV exposure, in 10 mM acetate, pH 5.4. (n=3)

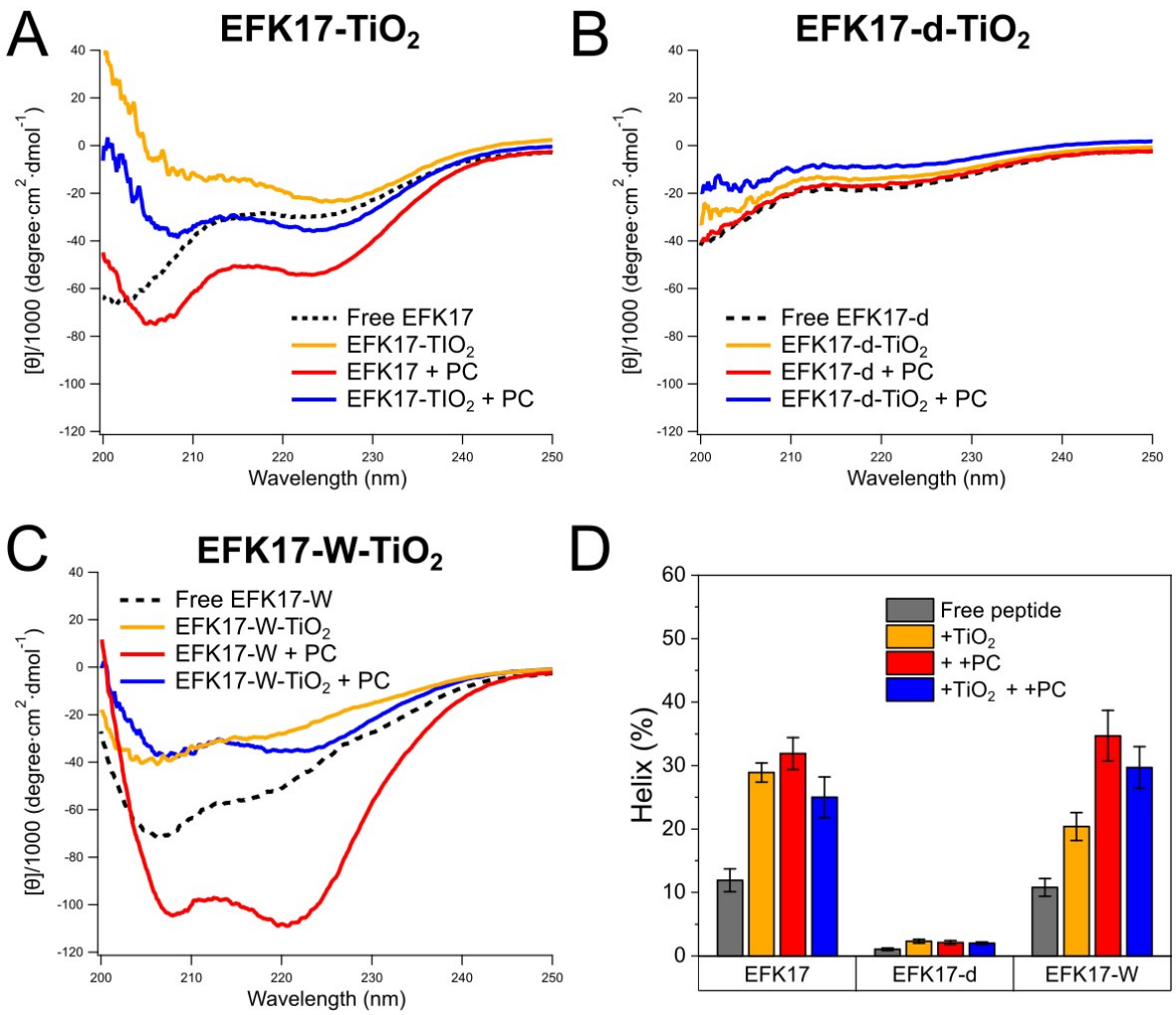

Figure S2. CD spectra of TiO_2 NPs coated with EFK17 (A), EFK17-d (B) and EFK17-W (C) in the absence and in the presence of **PC** LUVs. CD spectra of free peptides and peptides incubated with PC LUVs (in the absence TiO_2 NPs) are also included for comparison. Shown in (D) are results on alpha helix content (%) obtained from CD spectra fitting through the Bestsel method (7). All measurements were performed at 25°C, in 10 mM Acetate, pH 5.4. (n=3).

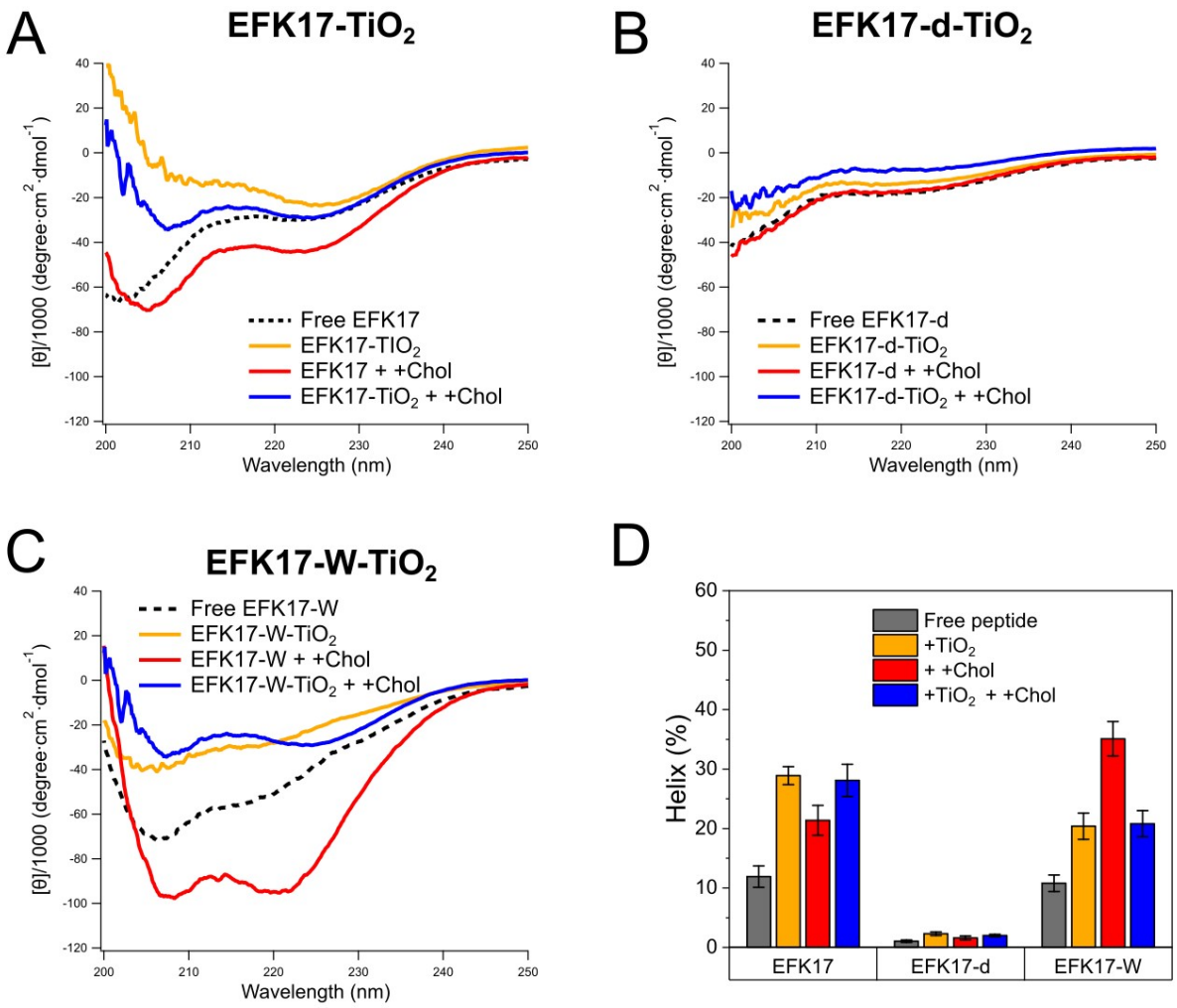

Figure S3. CD spectra of TiO_2 NPs coated with EFK17 (A), EFK17-d (B) and EFK17-W (C) in the absence and in the presence of **+Chol** LUVs. CD spectra of free peptides and peptides incubated with +Chol LUVs (in the absence TiO_2 NPs) are also included for comparison. Shown in (D) are results on alpha helix content (%) obtained from CD spectra fitting through the Bestsel method (7). All measurements were performed at 25°C, in 10 mM Acetate, pH 5.4. (n=3).

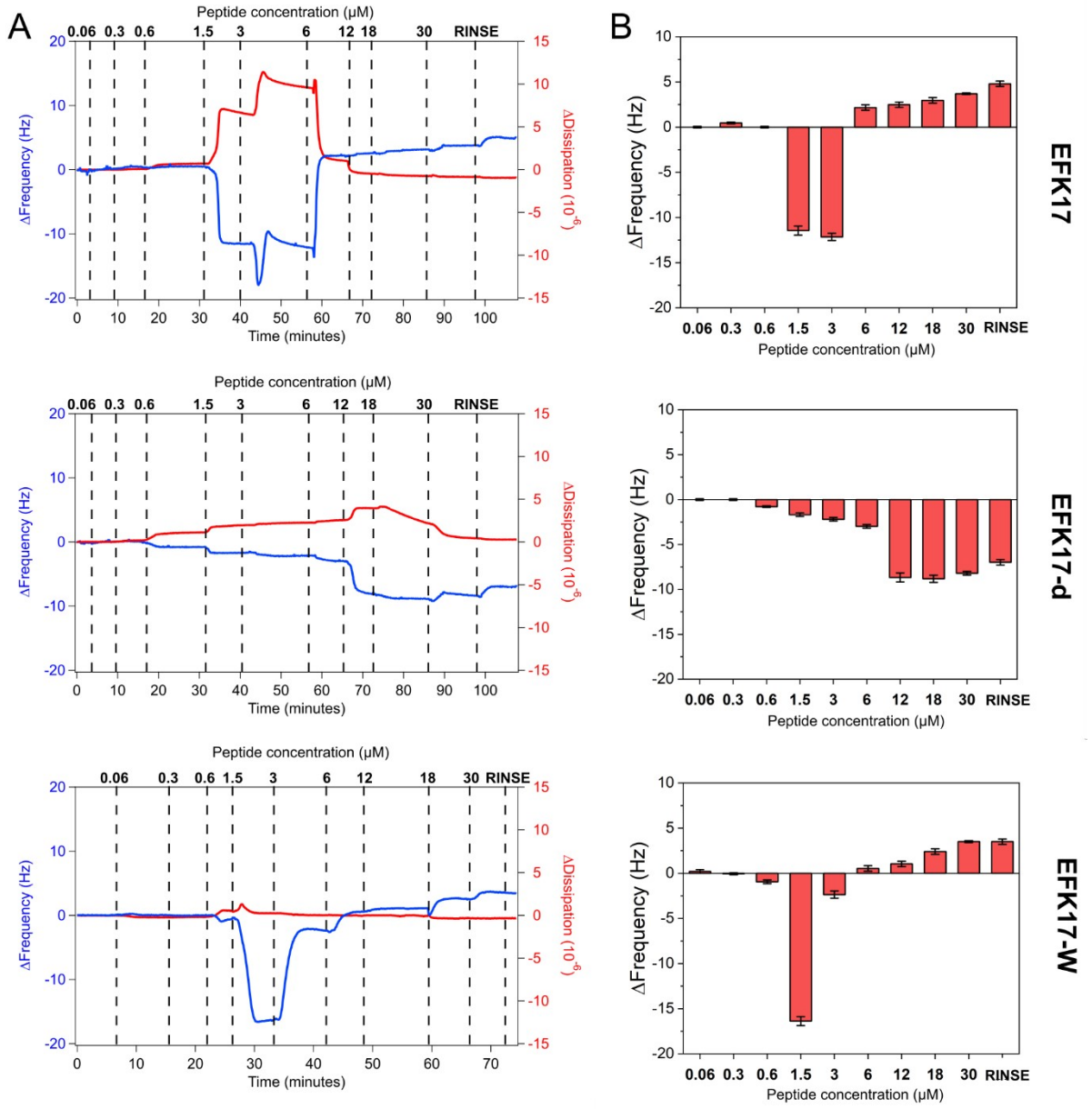

Figure S4. (A) Representative QCM-d profiles showing the 7th overtone of ΔFrequency (Hz) and ΔDissipation (·10^{-6}) changes during incubation of +PG with increasing concentrations of free EFK17 (top), EFK17-d (middle) and EFK17-W (bottom) in the range 0-30 μM, in 10 mM Acetate, pH 5.4. A final step of rinsing with buffer (in the absence of peptide) was also included to check peptide binding reversibility. (B) Corresponding ΔFrequency shifts (Hz) following the addition of free EFK17 (top), EFK17-d (middle) and EFK17-W (bottom) concentrations in the range 0-30 μM, in 10 mM Acetate, pH 5.4. (n=3)

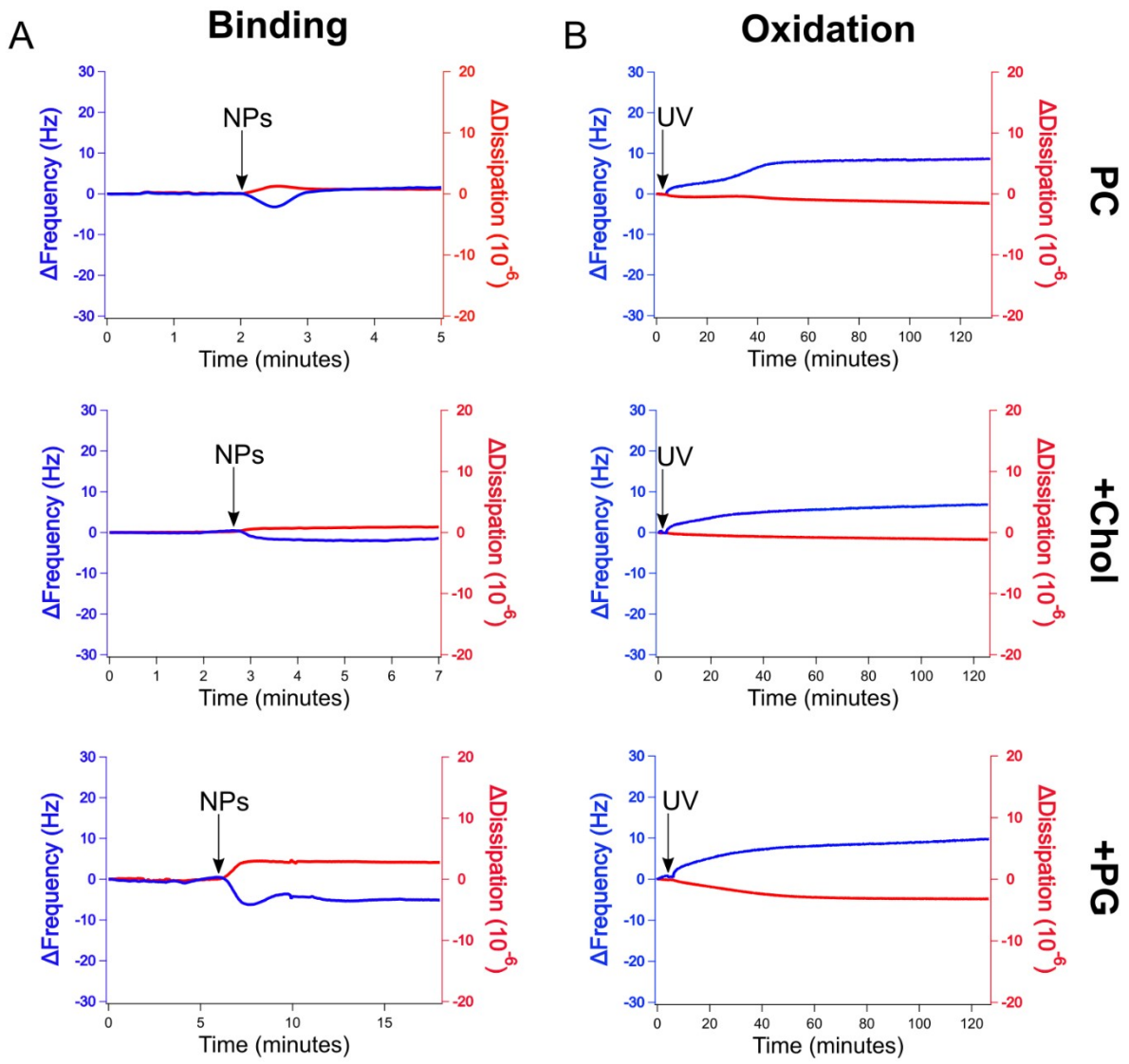

Figure S5. Representative QCM-d profiles showing the 7th overtone of ΔFrequency (Hz) and ΔDissipation (·10^{-6}) changes during (A) binding from 5 ppm **EFK17-TiO_2** to supported PC (top), +Chol (middle) and +PG (bottom) bilayers, as well as (B) effect of UV illumination, applied after rinsing with buffer and nanoparticle binding in 10 mM Acetate, pH 5.4. ΔF=0 and ΔD=0 correspond to Frequency and Dissipation shifts for the lipid bilayer right before NP binding (A) or UV illumination (B).

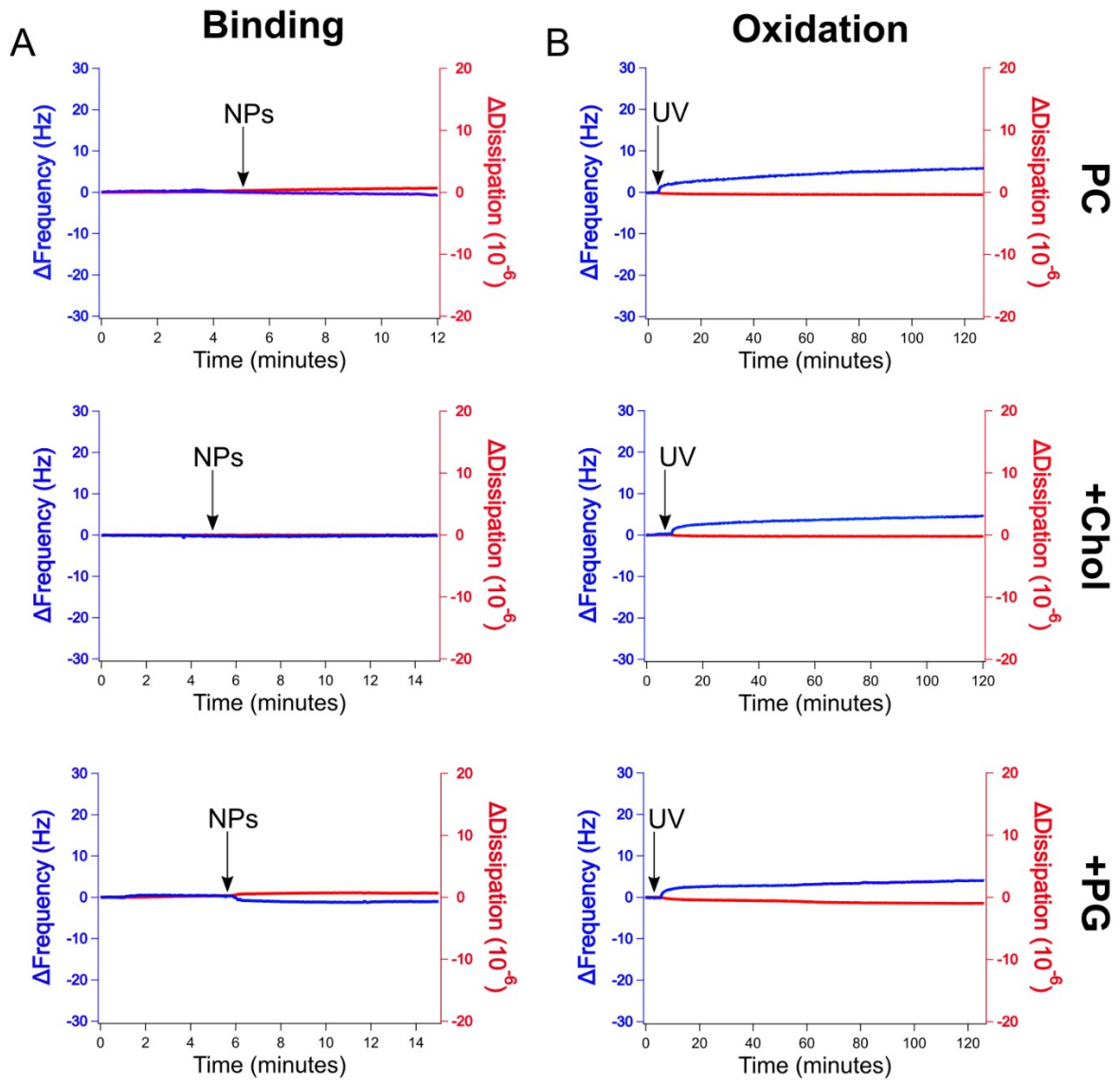

Figure S6. Representative QCM-d profiles showing the 7th overtone of ΔFrequency (Hz) and ΔDissipation ($\cdot 10^{-6}$) changes during (A) binding from 5 ppm **EFK17-d-TiO_2** to supported PC (top), +Chol (middle) and +PG (bottom) bilayers, as well as (B) effect of UV illumination, applied after rinsing with buffer and nanoparticle binding in 10 mM Acetate, pH 5.4. ΔF=0 and ΔD=0 correspond to Frequency and Dissipation shifts for the lipid bilayer right before NP binding (A) or UV illumination (B).

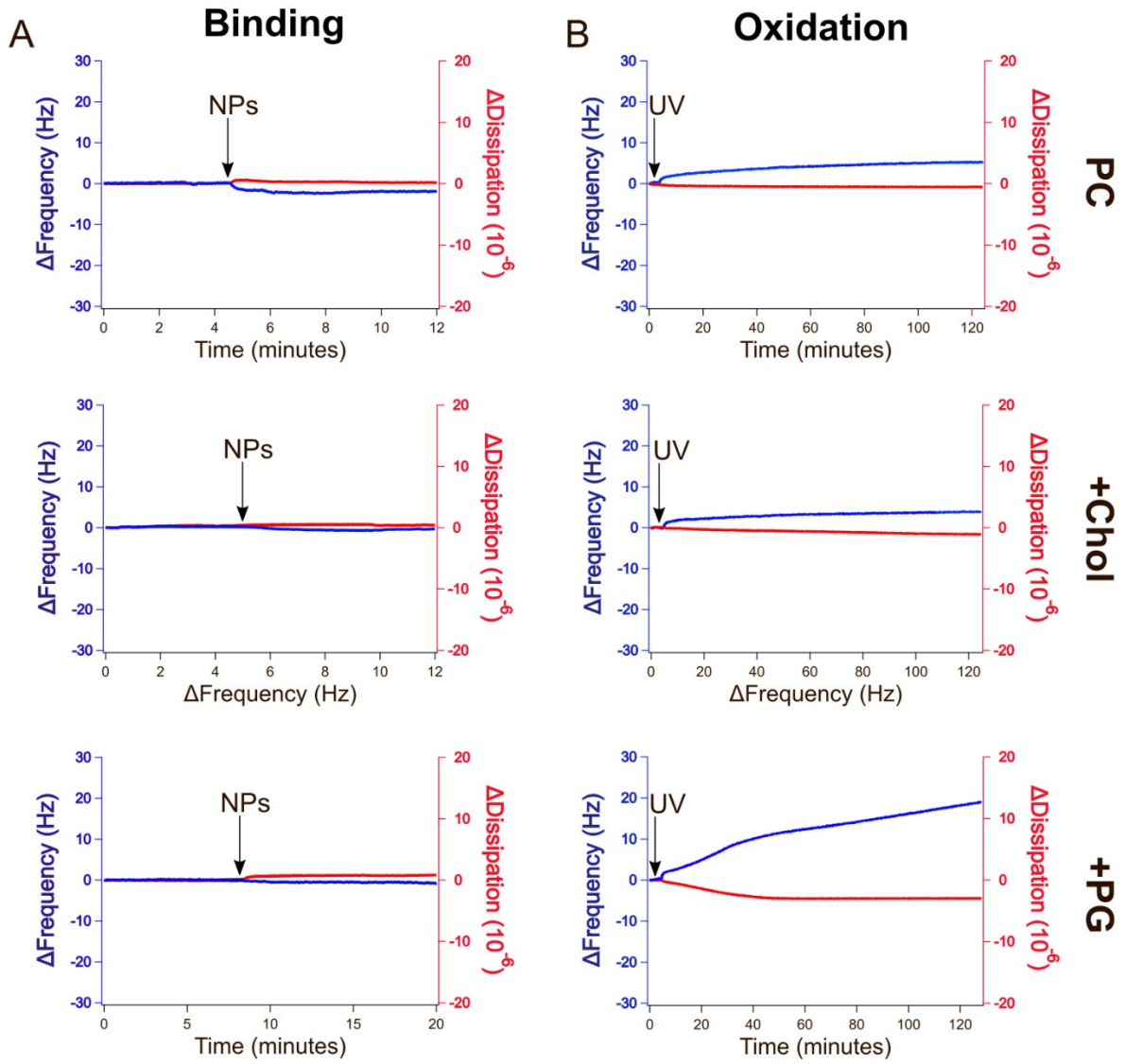

Figure S7. Representative QCM-d profiles showing the 7th overtone of ΔFrequency (Hz) and ΔDissipation (·10^{-6}) changes during (A) binding from 5 ppm **EFK17-W-TiO$_2$** to supported PC (top), +Chol (middle) and +PG (bottom) bilayers, as well as (B) effect of UV illumination, applied after rinsing with buffer and nanoparticle binding in 10 mM Acetate, pH 5.4. ΔF=0 and ΔD=0 correspond to Frequency and Dissipation shifts for the lipid bilayer right before NP binding (A) or UV illumination (B).

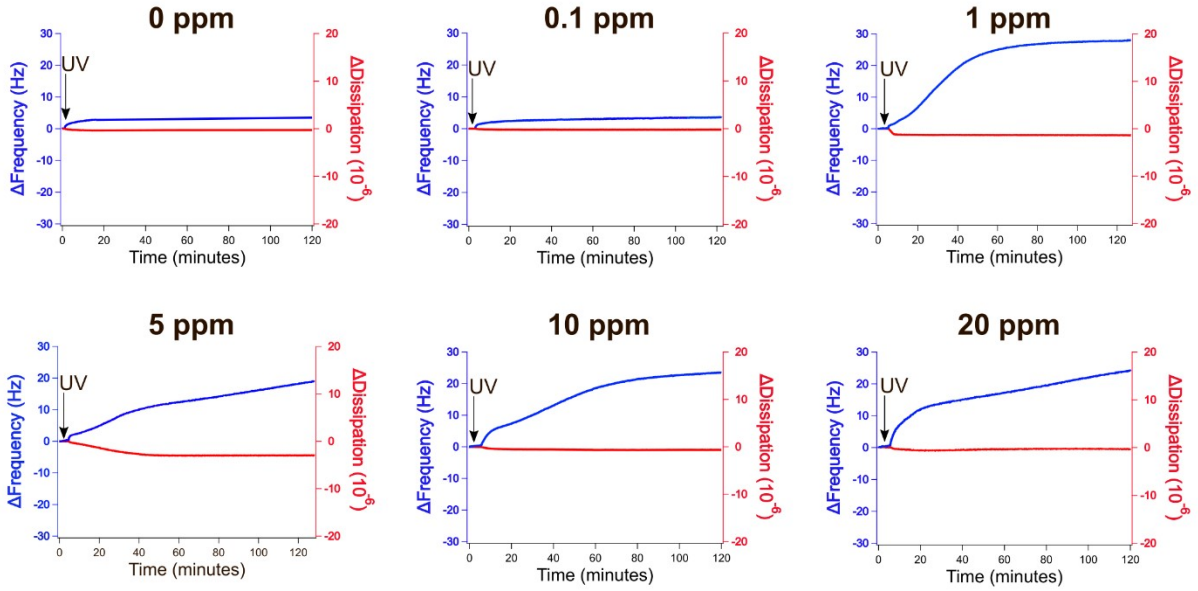

Figure S8. Representative QCM-d profiles showing the 7th overtone of ΔFrequency (Hz) and ΔDissipation ($\cdot 10^{-6}$) changes for supported +PG bilayers incubated with EFK17-W-TiO_2 at different concentrations (0-100 ppm), during *in situ* UV illumination, applied after rinsing with buffer and nanoparticle binding in 10 mM Acetate, pH 5.4. ΔF=0 and ΔD=0 correspond to Frequency and Dissipation shifts for the lipid bilayer right before UV illumination.

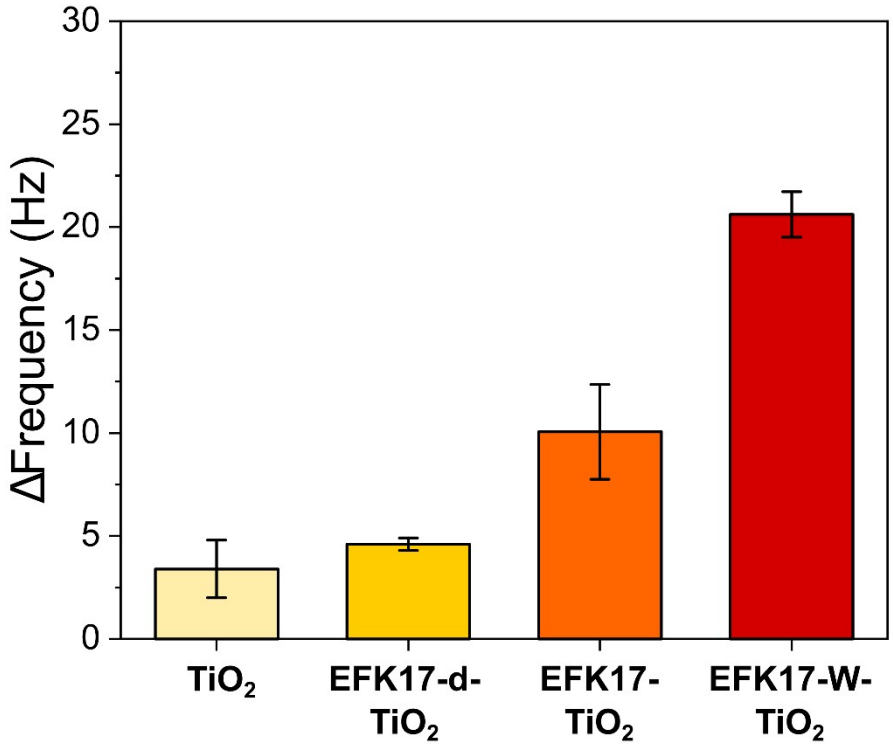

Figure S9. QCM-d results showing frequency shifts caused by 2 h of in situ UV illumination on +PG bilayers incubated with 5 ppm of bare TiO_2, EFK17-TiO_2, EFK17-d-TiO_2 and EFK17-W-TiO_2 NPs. ΔF=0 corresponds to the bilayer Frequency shift right before UV illumination. All measurements were performed in 10 mM Acetate, pH 5.4. (n=3).

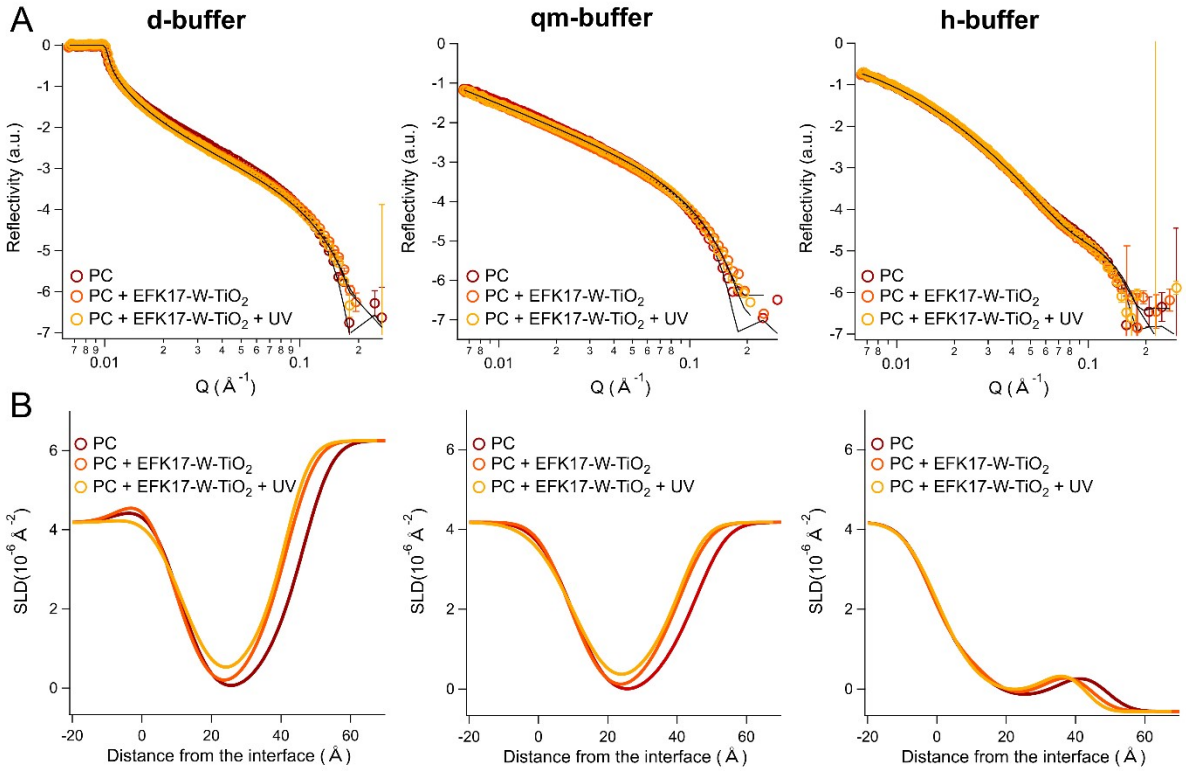

Figure S10. (A) NR curves with best model fits and (B) corresponding SLD profiles for supported **PC** bilayers before and after incubation with 20 ppm EFK17-W-TiO_2 NPs in d-buffer (left), qm-buffer (middle), and h-buffer (right). Shown also are reflectivity curves with best model fits and SLD profiles for the corresponding systems after 2 h of *in situ* UV exposure. All experiments were performed in 10 mM acetate, pH 5.4.

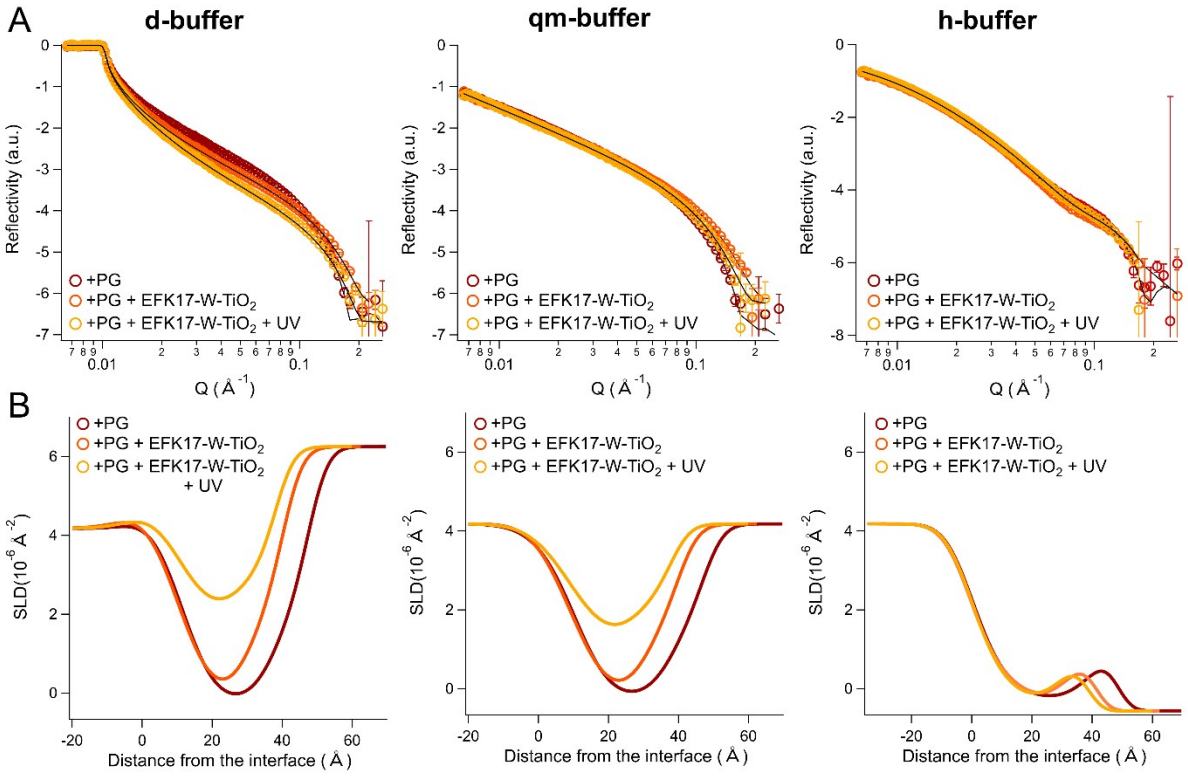

Figure S11. (A) NR curves with best model fits and (B) corresponding SLD profiles for supported **+PG** bilayers before and after incubation with 20 ppm EFK17-W-TiO_2 NPs in d-buffer (left), qm-buffer (middle), and h-buffer (right). Shown also are reflectivity curves with best model fits and SLD profiles for the corresponding systems after 2 h of *in situ* UV exposure. All experiments were performed in 10 mM acetate, pH 5.4.

References

1. Koenig, B. W. and Gawrisch, K. Specific volumes of unsaturated phosphatidylcholines in the liquid crystalline lamellar phase. BBA-Biomembranes 2005, 1715, 1, 65-70.

2. Kučerka, N., Tristram-Nagle, S., and Nagle, J.F. Structure of fully hydrated fluid phase lipid bilayers with monounsaturated chains. J. Membr. Biol. 2006**,** 208, 193-202.

3. Pabst, G., Danner, S., Karmakar, S., Deutsch, G., and Raghunathan, V.A. On the propensity of phosphatidylglycerols to form interdigitated phases. Biophys. J. 2007, 93, 513-525.

4. Nelson, A. Motofit – integrating neutron reflectometry acquisition, reduction and analysis into one, easy to use, package. J. Phys. Conf. Ser. 2010, 251, 012094.

5. Nelson, A. Co-refinement of multiple contrast neutron / X-ray reflectivity data using MOTOFIT. J. Appl. Cryst. 2006, 39, 273-276.

6. Heinrich, F., Ng, T., Vanderah, D.J., Shekar, P., Mihailescu, M., Nanda, H., and Lösche, M. A new lipid anchor for sparsely tethered bilayer lipid membranes. Langmuir 2009, 25, 4219-4229.

7. Micsonai, A., Wien, F., Kernya, L., Lee, Y. H., et al.. Accurate secondary structure prediction and fold recognition for circular dichroism spectroscopy. Proc. Nat. Acad. Sci. 2015, 112, E3095-E3103.